

The oscillations observed here may be related to those variations observed in very strong magnetic fields by Lawson *et al.*<sup>17</sup> and by Alvesalo.<sup>18</sup>

We wish to acknowledge helpful discussions or correspondence with M. C. Cross, A. J. Fetter, N. D. Mermin, T. L. Ho, K. Maki, H. E. Hall, B. R. Patton, and L. J. Sham.

\*Work supported by the U. S. Energy Research and Development Administration under Contract No. E(04-3)-34, P.A. 143.

<sup>1</sup>For theoretical background see A. J. Leggett, *Rev. Mod. Phys.* **47**, 331 (1975).

<sup>2</sup>For experimental background see J. C. Wheatley, *Rev. Mod. Phys.* **47**, 415 (1975).

<sup>3</sup>D. N. Paulson, M. Krusius, and J. C. Wheatley, *Phys. Rev. Lett.* **36**, 1322 (1976).

<sup>4</sup>N. D. Mermin and T. L. Ho, *Phys. Rev. Lett.* **36**, 594 (1976).

<sup>5</sup>M. C. Cross, *J. Low Temp. Phys.* **21**, 525 (1975).

<sup>6</sup>A. J. Leggett and S. Takagi, to be published.

<sup>7</sup>K. Maki and Ebisawa, *J. Low Temp. Phys.* **22**, 285 (1976).

<sup>8</sup>R. Combescot, *Phys. Rev. Lett.* **35**, 1646 (1975).

<sup>9</sup>G. E. Volovik, *Pis'ma Zh. Eksp. Teor. Fiz.* **22**, 234 (1975) [*JETP Lett.* **22**, 108 (1975)].

<sup>10</sup>P. W. Anderson and W. F. Brinkman, in *The Helium Liquids*, edited by J. G. M. Armitage and I. E. Farquhar (Academic, London, 1975), p. 315.

<sup>11</sup>M. Ishikawa, to be published.

<sup>12</sup>M. Shahzamanian, *J. Low Temp. Phys.* **21**, 589 (1975).

<sup>13</sup>P. Bhattacharyya, C. J. Pethick, and H. Smith, in *Proceedings of the Fourteenth International Conference on Low Temperature Physics, Otaniemi, Finland, 1975*, edited by M. Krusius and M. Vuorio (North-Holland, Amsterdam, 1975), Vol. 1, p. 9.

<sup>14</sup>S. Blaha, *Phys. Rev. Lett.* **36**, 874 (1976).

<sup>15</sup>M. C. Cross and P. W. Anderson, in *Proceedings of the Fourteenth International Conference on Low Temperature Physics, Otaniemi, Finland, 1975*, edited by M. Krusius and M. Vuorio (North-Holland, Amsterdam, 1975), Vol. 1, p. 29.

<sup>16</sup>M. C. Cross, private communication.

<sup>17</sup>D. T. Lawson, W. J. Gully, S. Goldstein, R. C. Richardson, and D. M. Lee, *J. Low Temp. Phys.* **15**, 169 (1974).

<sup>18</sup>T. Alvesalo, thesis, Helsinki University of Technology, 1974 (unpublished).

## Electric Field Breakdown of Charge-Density-Wave-Induced Anomalies in NbSe<sub>3</sub> †

P. Monçeau,\* N. P. Ong, and A. M. Portis

*Department of Physics, University of California, Berkeley, California 94720*

and

A. Meerschaut and J. Rouxel

*Laboratoire de Chimie Minérale A, 44037 Nantes Cedex, France*

(Received 1 June 1976)

We report the suppression by electric fields of longitudinal resistivity anomalies at 145 and 59 K in the compound NbSe<sub>3</sub>. Sample resistance was determined by conventional four-probe dc measurement as well as with short current pulses. We attribute the observed suppression to Zener breakdown across extremely small gaps introduced by the presence of charge density waves.

The anomalous electron transport properties of the transition-metal trichalcogenide, NbSe<sub>3</sub>, have recently been reported.<sup>1,2</sup> The dc resistivity shows two peaks in the vicinity of 129 and 49 K. These peaks have recently been observed also at microwave frequencies.<sup>3</sup> In this Letter we report the discovery that these anomalies are suppressed by relatively low applied electric fields. We associate these anomalies with gaps at the Fermi Surface (FS) as a result of the formation of charge density waves<sup>4</sup> (CDW), which have also been invoked to account for anomalies in the specific heat.<sup>2</sup> The measurements reported here

were carried out by conventional four-probe dc methods as well as with 5- $\mu$ sec pulses. Non-Ohmic behavior sets in with decreasing temperature below 145 K. The resistivity is observed to drop when the electric field exceeds relatively low values. The breakdown data agree remarkably well with an analysis based on Zener tunneling<sup>5</sup> across very small energy gaps of the order of 10<sup>-5</sup> eV. At the lower temperatures more than one gap is required to fit the measurements.

NbSe<sub>3</sub> crystallizes in the form of fibrous strands, which are easily separated. The structure has been determined by single-crystal x-ray

diffraction.<sup>6</sup> Six Se atoms form the vertices of a right triangular prism with a Nb atom at the center of the prism. Six prisms form the unit cell, which measures  $(10.006 \pm 0.005) \times (3.478 \pm 0.002) \times (15.626 \pm 0.008) \text{ \AA}^3$ . The distance between Nb atoms is  $3.478 \pm 0.002 \text{ \AA}$  along the  $b$  axis and varies from 4.45 to 4.25  $\text{ \AA}$  in the  $a$ - $c$  plane. The compound was formed by the direct reaction (without carrier) of Se and Nb in stoichiometric proportions. The mixture was sealed in quartz under vacuum and heated to  $700^\circ\text{C}$  for 15 days before quenching. Experimental determination of the composition of single crystals with a Castaing probe yielded for Nb, 28.61 and for Se, 71.39, which compares favorably with the theoretical values of Nb, 28.17, and Se, 71.83.

The samples used were typically  $7 \times 0.05 \times 0.01 \text{ mm}^3$  in size and were mounted on a quartz substrate inside a continuous-helium-gas-flow cryostat. Temperature stability was maintained to  $\pm 0.2 \text{ K}$  during the course of a measurement. Electrical contact was made to the samples with silver paint. Although the measurements reported here were performed with four probes, we have also obtained identical results with two and three probes. Also, our microwave conductivity measurements<sup>3</sup> are generally similar to the dc and pulsed measurements indicating that the contacts are Ohmic and that carrier injection is not important. Sample resistances ranged from 10 to  $70 \text{ } \Omega$  at room temperature. In the pulsed experiment, pulses of  $5\text{-}\mu\text{sec}$  duration and  $10\text{-nsec}$  rise time were displayed on a storage oscilloscope. Increasing the pulse width by an order of magnitude did not change the voltage measured at any temperature. Typically the temperature was held constant, and the voltage drop was measured for the full range of current densities. For current densities below  $10 \text{ A mm}^{-2}$  the dc technique was used. Self-heating of the sample became important above this value, and the pulsed technique extended the measurements to  $100 \text{ A mm}^{-2}$ . The possibility that the observed non-Ohmic behavior is due to microheating of the sample induced by marked current inhomogeneity has been investigated theoretically. It can be shown that microdomains relax too fast to cause measurable temperature inhomogeneities. Current densities above  $150 \text{ A mm}^{-2}$  were found to cause irreversible changes in sample resistance, probably because of contact damage.

Figure 1 shows the suppression of the high-temperature peak. Above  $145 \text{ K}$  Ohmic behavior is rigorously maintained. The phase transition

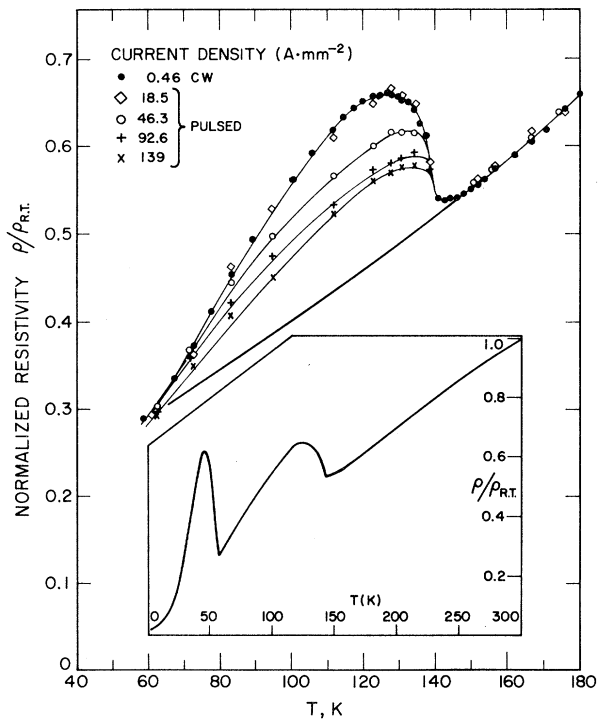


FIG. 1. The normalized resistivity as a function of temperature at five current densities near the higher resistivity anomaly. The heavy line represents the limiting resistivity with available electric fields. CW represents measurements with dc current. The inset shows the normalized low-current resistivity for the full temperature range.

occurs at the same temperature,  $145 \text{ K}$ , for all four current densities. In Fig. 2 data for the lower resistivity anomaly are shown. As in the higher-temperature anomaly, the transition occurs at the same temperature  $59 \text{ K}$  at all current densities. However, the suppression of the lower peak is more dramatic. A 50% reduction requires only  $3 \text{ A mm}^{-2}$  compared to  $90 \text{ A mm}^{-2}$  for the higher peak. The effects of self-heating are evident for the highest dc current densities. The dashed curve (for dc  $37.38 \text{ A mm}^{-2}$ ), for example, lies considerably above the rest of the data at  $60 \text{ K}$ . It agrees with the other data if it is shifted by up to  $15 \text{ K}$  to the right, indicating that the sample is  $15 \text{ K}$  warmer than the bath at  $60 \text{ K}$ . No such shift occurs at the highest pulsed current density ( $100 \text{ A mm}^{-2}$ ). Results from measurements on four different samples show the same behavior and give the same breakdown field at each temperature.

The suppression of both resistivity anomalies in  $\text{NbSe}_3$  has also been achieved by applying pressure.<sup>2</sup> In the pressure experiments both the peak

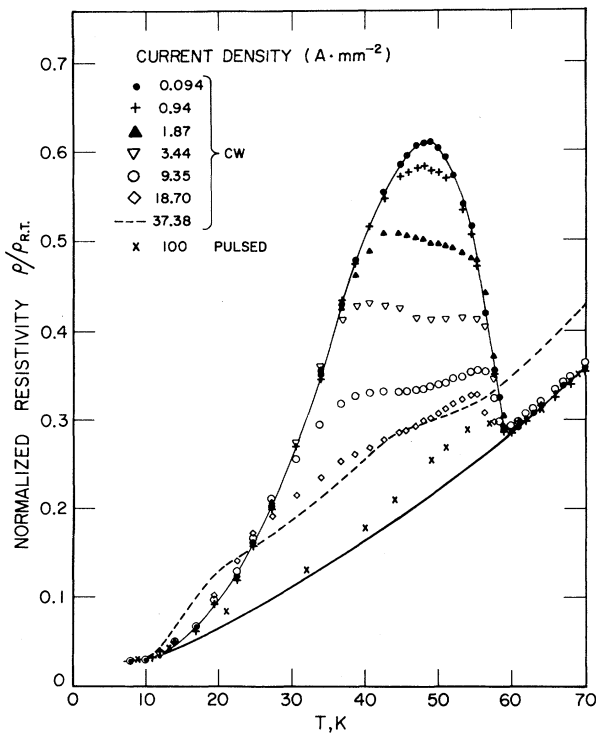


FIG. 2. The normalized resistivity as a function of temperature near the lower resistivity anomaly at seven current densities. The dashed line shows the effect of Ohmic heating at the highest dc current density. The heavy line represents the limiting resistivity with available electric fields.

temperature and the amplitude of the lower resistivity anomaly rapidly decrease with pressure. The lower peak is completely removed at a pressure of 6 kbar, while the upper peak is reduced by 30% at 4 kbar. In this respect, the peak suppression by pressure is similar to what has been observed in  $\text{NbSe}_2$ , where it has been shown that charge density waves are responsible for the small resistivity anomaly at 33.5 K and ambient pressure.<sup>7</sup> The evidence for similar existence of CDW's in  $\text{NbSe}_3$  is strong, although not conclusive. The specific heat also shows an anomaly<sup>2</sup> at 50 K in  $\text{NbSe}_3$  similar to that in  $\text{NbSe}_2$ <sup>8</sup> and consistent with theoretical considerations based on a CDW model.<sup>9</sup> An effort is being made to observe the CDW's directly by diffuse x-ray scattering.

The pressure dependence of the critical temperature of the resistivity anomalies in  $\text{NbSe}_3$  referred to above is consistent with a CDW interpretation. In particular, the increase in strain energy as well as the shift in FS caused by applying pressure decrease the critical tempera-

ture  $T_c$  for CDW formation.<sup>7</sup> In contrast, the breakdown of resistivity anomalies by applied electric fields reported here does not affect  $T_c$ . The field affects the nonequilibrium properties of the sample, whereas the pressure alters the equilibrium state. Below  $T_c$  gaps open up at portions of the FS changing its area and topology and leading to an increase in resistivity. Increasing the electric field induces Zener tunneling across these gaps. At sufficiently high fields the effect of these gaps on transport properties may be completely removed although superlattice structure persists. Using the familiar electric breakdown equation,<sup>5</sup> the conductivity may be written as

$$\sigma(T, E) = \sigma_0(T) + \sum_n \sigma_n(T) \exp[-E_{0n}(T)/E], \quad (1)$$

$$E_{0n}(T) = \pi \Delta_n^2(T) / |e| \hbar v_n, \quad (2)$$

where the sum in Eq. (1) is over the gaps,  $\Delta_n$  is the  $n$ th half-gap energy, and  $v_n$  is the component of the carrier velocity normal to the superlattice Bragg reflection plane at the FS in the absence of the  $n$ th gap.

$\text{NbSe}_3$  undergoes two phase transitions. At 145 K a gap opens at the FS giving rise to the first anomaly. Below the second critical temperature 59 K a new gap opens and causes the second larger anomaly. In the vicinity of the high-temperature anomaly at 123 K the data can be remarkably well fitted with Eq. (1) up to the highest applied field with just one term in the sum. We have

$$\sigma(T, E) = \sigma_0(T) + \sigma_3(T) \exp(-E_{03}/E) \quad (T \sim 123 \text{ K}). \quad (3)$$

Similarly at 54 K the breakdown data can be equally well fitted with one term in the form of Eq. (3) with  $\sigma_3$  and  $E_{03}$  replaced by  $\sigma_2$  and  $E_{02}$ . At 49 and 40 K two terms are required in the sum to give agreement with experiment. Labeling the additional term by subscript 1, we write

$$\sigma(T, E) = \sigma_0(T) + \sigma_1(T) \exp(-E_{01}/E) + \sigma_2(T) \times \exp(-E_{02}/E) + \dots \quad (T < 50 \text{ K}). \quad (4)$$

We stress that the term labeled by subscript 3 in Eq. (3) *should* appear in Eq. (4). However,  $E_{03}$  has increased to the extent that Zener tunneling across the associated gap is no longer possible at available fields, and our data do not give an indication of  $E_{03}$  below 50 K. We show in Fig. 3 a semilogarithmic plot of the field-induced conductivity as a function of inverse applied electric field. The curves follow from Eqs. (3) and (4)

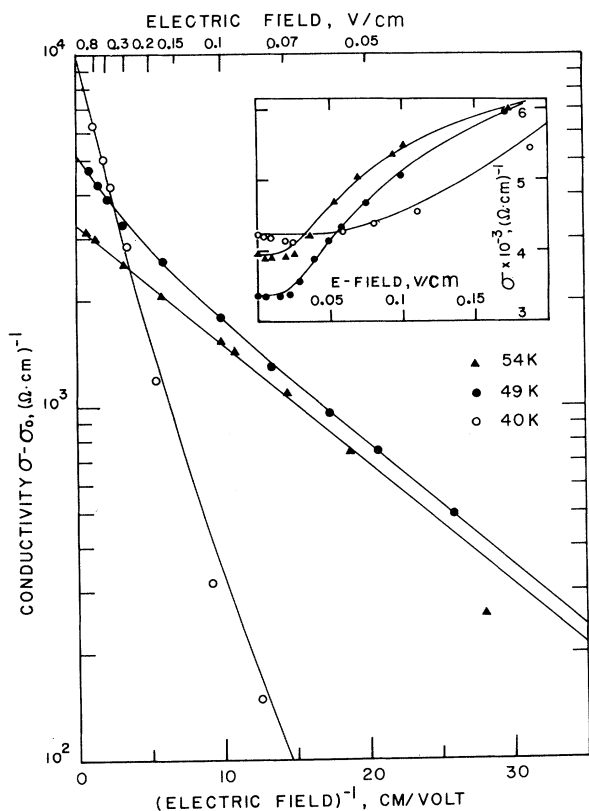


FIG. 3. The fit of experimental data by Zener tunneling analysis. The solid lines are the best fit to the data using Eq. (1) at three temperatures near the lower anomaly. Inset shows the total conductivity versus electric field in the low-field limit.

with  $E_{01}$ ,  $E_{02}$ , and  $E_{03}$  as parameters.

Assuming a velocity at the FS of  $v = 10^7$  cm sec $^{-1}$  we compute a half-gap at 123 K of  $5.4 \times 10^{-5}$  eV (0.63 K) and at 54 K of  $1.3 \times 10^{-5}$  eV (0.15 K). These extremely small gaps are quite incompatible with a BCS-type relation:

$$\Delta = 1.7kT_c. \quad (5)$$

For  $T_c = 145$  K, Eq. (5) requires  $\Delta_3 \sim 2 \times 10^{-2}$  eV, which is three orders of magnitude larger than the measured value. However, if both  $s$  and  $d$  electrons are present in NbSe $_3$ , as in the case of Cr, $^{10,11}$  then the  $d$ -electron FS drives the superlattice phase transition while the  $s$  electrons dominate the transport properties. The weaker coupling of  $s$  electrons to the CDW would result in a much smaller gap than given by Eq. (5), and it may be possible to account in this way for the discrepancy in gap size.

It is at first sight surprising that a gap much smaller than  $kT$  can so strongly modify the con-

ductivity, particularly since the probability that a state is occupied can be little affected by the presence of such small gaps. In the absence of phonon excitation across the gaps, the origin of the anomalies is clear. And since phonon excitations induce transitions in both directions they cannot produce a predominance of carriers above the gap as required to suppress the anomalies. On the other hand, an electric field large enough to induce tunneling can do precisely this.

We are indebted to Professor L. M. Falicov for pointing out to us the similarity between the behavior of NbSe $_3$  and of chromium and for suggesting that our observed reduction in resistivity at high electric fields was associated with Zener breakdown. We would like to thank Thomas Hsiang for the loan of equipment, and acknowledge help from Eugene Sanders in pulse electronics.

†Work supported in part by the National Science Foundation through the Division of Materials Research, Grant No. 75-23018.

\*Permanent address: Centre de Recherches sur les Très Basses Températures, Centre National de la Recherche Scientifique B. P. 166, 38042 Grenoble, France.

<sup>1</sup>P. Haen, P. Monceau, B. Tissier, G. Waysand, A. Meerschaut, P. Molinie, and J. Rouxel, in *Proceedings of the Fourteenth International Conference on Low Temperature Physics, Otaniemi, Finland, 1975*, edited by M. Krusius and M. Vuorio (North-Holland, Amsterdam, 1975), Vol. 5, p. 445.

<sup>2</sup>J. Chaussy, P. Haen, J. C. Lasjaunias, P. Monceau, G. Waysand, A. Waintal, A. Meerschaut, P. Molinie, and J. Rouxel, to be published.

<sup>3</sup>N. P. Ong, P. Monceau, and A. M. Portis, to be published.

<sup>4</sup>J. A. Wilson, F. J. DiSalvo, and S. Mahajan, *Adv. Phys.* **24**, 117 (1975).

<sup>5</sup>J. M. Ziman, *Principles of the Theory of Solids* (Cambridge Univ. Press, Cambridge, England, 1972), 2nd ed., Sect. 6.8.

<sup>6</sup>A. Meerschaut and J. Rouxel, *J. Less-Common Metals* **39**, 197 (1975). A report by E. Revolinsky, G. A. Spiering, and D. J. Beerntsen, *J. Phys. Chem. Solids* **26**, 1029 (1965), of the observation of NbSe $_3$  was later corrected to NbSe $_4$ . See E. Revolinsky, B. E. Brown, D. J. Beerntsen, and C. H. Armitage, *J. Less-Common Metals* **8**, 63 (1965). See also the review by K. Selte, E. Bjerkelund, and A. Kjekshus, *J. Less-Common Metals* **11**, 14 (1966).

<sup>7</sup>R. Delaplace, P. Molinie, and D. Jerome, *J. Phys. (Paris)*, *Lett.* **37**, L13 (1976); C. Berthier, P. Molinie, and D. Jerome, *Solid State Commun.* **18**, 1393 (1976).

<sup>8</sup>J. M. E. Harper, T. H. Geballe, and F. J. DiSalvo,

Phys. Lett. **54A**, 27 (1975).<sup>9</sup>W. L. McMillan, Phys. Rev. B **12**, 1187, 1197 (1975).<sup>10</sup>A. L. Trego and A. R. Mackintosh, Phys. Rev. **166**,

495 (1968).

<sup>11</sup>L. M. Falicov and M. J. Zuckermann, Phys. Rev. **160**, 372 (1967).

## Inelastic Resonant Transitions of Atoms on a LiF Surface

P. Cantini, G. P. Felcher,\* and R. Tatarek

Gruppo Nazionale di Struttura della Materia del Consiglio Nazionale delle Ricerche, and Istituto di Scienze Fisiche dell'Università, Genova, Italy

(Received 3 May 1976)

New results of He and Ne atomic beams scattered from the (001) face of LiF are presented. The angular distribution of the inelastically scattered intensity shows pronounced minima that are identified with the occurrence of bound-state resonances for inelastic processes. The extent to which the effect can be used to determine the phonon spectrum at the surface is discussed.

It has been suggested<sup>1,2</sup> that inelastic scattering of atomic beams from crystal surfaces could be one of the most useful tools to investigate surface phonons. Most of the measurements made hitherto employed the diffraction method, where the intensity of the non-Bragg-scattered beam was measured; whenever structure in the scattered distribution appeared, it was correlated with some feature of the phonon spectrum.<sup>2-4</sup>

We present detailed measurements of this type on the (001) face of LiF, in order to show that the inelastic reflection probability is strongly affected by the presence of bound-state resonances, which play a more important role than hitherto recognized in the scattering process of atoms from a surface. We have attempted to use the selective character of the inelastic resonances to analyze the excitation spectrum at the surface.

For one-phonon inelastic processes the usual conservation rules of energy and momentum for a gas atom of mass  $M$ , incident with a wave vector  $\vec{k}_i = (\vec{K}_i, k_{iz})$  and scattered from a surface at  $z=0$ , with an outgoing wave vector  $\vec{k}_f = (\vec{K}_f, k_{fz})$ , are

$$k_f^2 = k_i^2 \pm 2M\omega/\hbar, \quad \vec{K}_f = \vec{K}_i + \vec{G} \pm \vec{Q}, \quad (1)$$

where  $\vec{G}$  is a surface reciprocal-lattice vector and  $\omega$  and  $\vec{Q}$  are the phonon frequency and momentum parallel to the surface respectively.

In the diffraction method, the angular distribution of the scattered intensity  $I(\Omega_f)$  is proportional to

$$\int (d^3R/d\omega d^2\Omega) d\omega \quad (2)$$

or to an integral of the reflection probability ( $d^3R/d\omega d^2\Omega$ ) along a line  $\omega'(\vec{Q})$  which is defined by Eqs.

(1) for a given incident wave vector  $\vec{k}_i$  and a final direction  $\Omega_f$ .

The detected atoms are inelastically scattered by phonons whose surface-projected dispersion function  $\omega = \omega_s(\vec{Q})$  crosses the line  $\omega'(\vec{Q})$ ; this line, for in-plane scattering, is the parabola

$$\pm 2M\omega'/\hbar = k_i^2 - (\vec{K}_i + \vec{G}_{m,n} \pm \vec{Q})^2/\sin^2\theta_f. \quad (3)$$

In Fig. 1 the lowest part of the excitation spectrum of the (001) face of LiF is sketched and  $\omega'(\vec{Q})$  is drawn for scattering in the (100) plane, around the (0,0) peak. The lowest acoustic branch

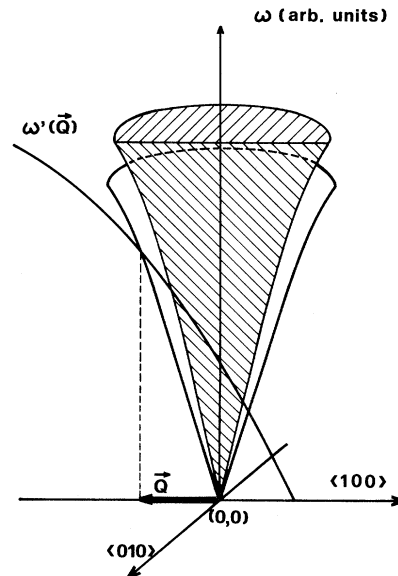


FIG. 1. Lowest part of the surface-projected dispersion function at the (001) face of LiF, around the (0,0) reciprocal vector.  $\omega'(\vec{Q})$  is an integration line for the intensity scattered at a certain angle  $\theta_f$  in the  $\langle 100 \rangle$  azimuth.